Actas de las XXXIX Jornadas de Automática, Badajoz, 5-7 de Septiembre de 2018
https://doi.org/10.17979/spudc.9788497497565.0731

Simplified model of ureteral peristalsis bolus using fluid structure interaction

Enrique Mancha Sánchez
Centro de Cirugía de Mínima Invasión Jesús Usón, emancha@ccmijesususon.com

Juan Carlos Gómez Blanco
Centro de Cirugía de Mínima Invasión Jesús Usón, jcgomez@ccmijesususon.com

Julia Estíbaliz De la Cruz Conty
Centro de Cirugía de Mínima Invasión Jesús Usón, jecruz@ccmijesususon.com

Francisco Miguel Sánchez Margallo
Centro de Cirugía de Mínima Invasión Jesús Usón, msanchez@ccmijesususon.com

José Blas Pagador Carrasco
Centro de Cirugía de Mínima Invasión Jesús Usón, jpagador@ccmijesususon.com

Federico Soria Gálvez
Centro de Cirugía de Mínima Invasión Jesús Usón, fsoria@ccmijesususon.com

Abstract

Current computational models of ureter are not usually based on physiological behaviour of anatomical structures. For this reason, we propose a new simplified model of ureteral flow to simulate a peristalsis bolus on the distal section of the ureter. This model uses a closed ureter that generates the urinary bolus with an expansive force applied in its wall. To analyse this, a computational FSI simulation is proposed to recreate the peristalsis movement of the ureter in its distal section. These preliminary results will be improved in future works to build a more complex model and to analyse the effects in the urine flow of a new design of a half-length ureteral stent.

Keywords: Computational simulation, ureter, FSI, peristalsis

1 INTRODUCTION

Urine flows from the renal pelvis to the urinary bladder in healthy people through the ureter for two reasons: a physiological activity (peristalsis) and a physical phenomenon (pressure gradient in an open system). Peristalsis consists in the transport of urine in isolated boluses along the ureter. The movement of each bolus is driven by a cell to cell contraction and expansion. This movement is assume to be a wave that moves continuously along the ureter [1].

In urinary tract research, ureteral flow is one of the major topics to investigate. There are works that tries to explain the ureter movement looking to their mechanical properties [2],[3]. Other research pathway is performing computational simulations. These simulations can be divided into 1) flow in stented ureters and 2) peristalsis flow. Stented ureters have a completely different behaviour compared to non-stented ureters. These ureters have no peristalsis due to the loss of muscle tone and works under the same principle as a straight tube. Some examples of this research, such as Cummings [4], Siggers [5] or Gómez-Blanco [6], study the urine flow through a stented ureter performing 2D axisymmetrical or 3D CFD (Computational Fluids Dynamics) or FSI (Fluid-Structure Interaction) simulations. This work presents a new simplified computational model of the ureteral peristalsis that will be used in future complex simulations of a new stent design. This new stent design ends in the middle length of the ureter, so it allows the ureter to have a peristalsis movement in the distal part.

Peristalsis flow has still room for improvement in computational simulations due to the complexity of the model. Some works use CFD axisymmetric flow [7], [8], while others consider FSI approaches [9], [7], but the reliability of the computational model really depends on the peristalsis wave definition. In this sense, there are some approaches to define the peristaltic wave: 1) contraction pressure distribution [8] applied in the ureter or 2) solid wall moving along the ureter [10], [7].

However, very few efforts have been focused on controlled displacement [9], or expansive forces in the ureter [11]. It is important to note that the physiological movement of a bolus in the ureter is an expansion of the lumen [12]. This means that the ureteral lumen is closed and the ureter wall starts to expand when the renal pelvis reaches a certain pressure performing the urinary bolus.

Hence, the main objective of this work is to analyse the flow in a peristaltic bolus performing a computational simulation but creating the peristalsis bolus by the applying of an expansion volumetric force in the ureter wall.

2 METHODS

2.1 MODEL

Our simplified model of the ureter was designed and simulated in COMSOL Multiphysics through an axisymmetric 2D model. A distal section of the ureter (non-stented section of that future complex model) was modeled with 100 mm length, 3 mm wall width and 0.5 mm lumen. After that, a FSI simulation was run. For this simulation, urine was considered such as Newtonian, incompressible fluid and the flow was assumed as laminar. The density (993.3 kg/m^3) and the dynamic viscosity (0.6913 cP) of urine were considered equal to those of water at 37 °C. The solid domain used in this model was not taken into account in the results due to the simulation protocol. The solid domain has been used to generate a certain displacement in the fluid by the application of a volumetric force.

2.2 GOVERNING EQUATIONS

For the fluid domain, according to our Newtonian and incompressible urine, the incompressible Navier-Stokes continuity and momentum equations are given:

$$\rho \nabla \cdot u_{fluid} = 0 \tag{1}$$

$$\rho \frac{\partial u_{fluid}}{\partial t} + \rho (u_{fluid} \cdot \nabla) u_{fluid} = \nabla \cdot [-\rho I + \mu (\nabla u_{fluid} + (u_{fluid})^T)] + F \tag{2}$$

where F is the external force applied on the fluid. In this simulation, the external force is generated by the deformation of the solid domain, interacting with the fluid domain due to the coupled physics of FSI.

For the solid domain, the equilibrium equation is given by:

$$\rho \frac{\partial^2 u_{solid}}{\partial t^2} - \nabla \cdot \sigma = F_V \tag{3}$$

where σ is the Cauchy stress tensor, F_V the body force and u_{solid} the deformation of the solid. Cauchy stress tensor is calculated from the second Piola-Kirchhoff stress S by:

$$\rho = J^{-1} F S F^T \tag{4}$$

where F, the deformation gradient, can be expressed in terms of the gradient of displacement vector u_{solid} as:

$$F = (I + \nabla u_{solid}) \tag{5}$$

where I is the identity matrix and J is the Jacobian of the deformation given by:

$$J = det(F) \tag{6}$$

the linear elastic material strain tensor ϵ is written in terms of the displacement gradient:

$$\epsilon = \frac{1}{2}[(\nabla u_{solid})^T + \nabla u_{solid} + (u_{solid})^T u_{solid}] \tag{7}$$

Hooke s law relates the stress tensor, the strain tensor and temperature as it follows:

$$s = s_0 + c : (\epsilon - \epsilon_0 - \epsilon_{th}) \tag{8}$$

Where c is the 4^{th} order elasticity tensor, : stands for the double-dot tensor product, s_0 and ϵ_0 are initial stresses and strains, $\epsilon_{th} = \alpha(T - T_{ref})$ is the thermal strain and $\alpha$is the coefficient of thermal expansion.

For the FSI physic it is used an arbitrary Lagrangian-Eulerian (ALE) method to solve solid and fluid domains [13]. The total force exerted on the solid boundary by the fluid is:

$$f_r = n \cdot [-pI + \mu (\nabla u_{fluid} + (\nabla u_{fluid})^T)] \tag{9}$$

where, n is the outward normal to the boundary. The volumetric force at the solid domain is given by:

$$F_V = \rho \frac{\partial^2 u_{solid}}{\partial t^2} - \nabla \cdot \sigma \tag{10}$$

where F_V is the volumetric force, but it is calculated by:

$$F_V = \frac{F_{tot}}{V} \tag{11}$$

where F_{tot} is the applied force and V the volume of the solid domain. A transformation of the force is necessary to couple spatial frame (Navier-Stokes equations) and material frame (Solid mechanics interface), this is done according to:

$$F = f \frac{dv}{dV} \tag{12}$$

where dv and dV are the mesh element scale factors for the spatial frame and the material frame. Also, velocity of the moving wall and fluid velocity has to be coupled:

$$u_{fluid} = u_w \tag{13}$$

where, the solid displacement change rate consists of the structural velocities:

$$u_w = \frac{\partial u_{solid}}{\partial t} \tag{14}$$

2.3 DOMAINS

Fluid domain. Urine was the liquid used for the fluid domain and it was considered such as incompressible and Newtonian fluid (similar to water). Density was set as $\rho = 993.3 kg/m^3$ and viscosity as $\mu = 0.6913 cP$. Inlet and outlet boundary were set as open boundary condition, so fluid can enter and leave the domain freely. In this way, only the movement of the wall, produced by the peristaltic force applied, was the responsible of the impulsion of the fluid.

Solid domain. In this model the ureter wall was set as linear elastic material, not as hyperelastic material as described in previous studies [14]. A volumetric force was applied in the ureter solid domain radial axis, r, as described in 11, being F_{tot}:

$$F_{tot} = Amp \cdot \left[\left| sin\left(\frac{\pi}{8} + \pi \cdot \frac{z - Vt}{Lam}\right)\right| - sin\left(\frac{pi}{8} + \pi \cdot \frac{z - Vt}{Lam}\right)\right] \tag{15}$$

where Amp was the amplitude of the force applied, V the movement speed of the peristaltic bolus, Lam the wavelength and z was the longitudinal axis. These parameters were set-up to $9 \cdot 10^7$ N (Amp), 20 mm/s (V) and 30 mm (Lam).

2.4 MESH

A 2D triangular and quadrilateral element mesh was created for this simulation. Quadrilateral elements were created for the boundary of fluid domain and it consists of 1626 elements. Triangular elements were in the remaining unmeshed geometry of both domains (15292 elements). It shows a 0.8586 mean quality of elements with a 0.5027 of minimal quality of elements.

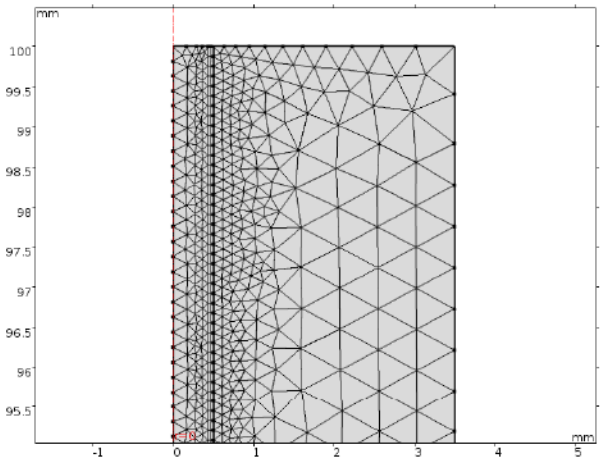

Figure 1: Mesh zoom of both domains

2.5 SIMULATION

Simulation was carried out with a time-dependent study, with a fully coupled solver. Simulation time was between 0 and 1.5 s with a time step of 10 ms. Solver used was a fully coupled solver that used MUMPS as a linear solver with a non-linear method with an automatic dumping factor.

3 RESULTS AND DISCUSSION

3.1 MOVEMENT

The movement of the fluid boundary in the 1.5 s simulation, obtained by the application of the

volumetric force on the solid domain, is shown in Figure 2. This wave represents the movement of the urinary bolus along the ureter. It can be seen that the maximum height reached is 1.8 mm and there is no displacement of the ureter between each bolus. The waveform is simulated as a sinusoidal wave as other researchers have done [9]. In our study the initial geometry needs a rectified sinusoidal to generate a correct peristalsis representation. It is clear that the peristalsis movement cannot be simulated with a simple sinusoidal wave.

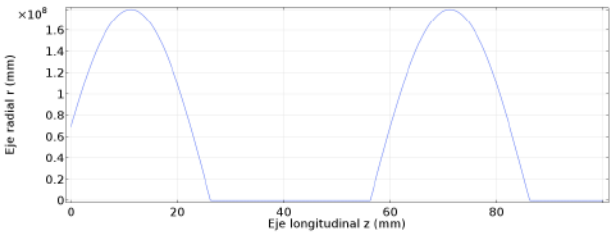

Figure 2: Radial displacement at simulation time of 1.5 s along the longitudinal axis

3.2 VELOCITY

Velocity profile can be seen in Figure 3 that shows two main facts occurring when the bolus moves. First, the velocity increases when the ureter expands to form the urinary bolus. Later, another increase of the velocity appears when the ureter comes back to its initial state. The expansion and the contraction of the ureter wall provoke a urine flow in the direction of the movement of the bolus. Maximum velocities are placed where the bolus starts (4.95 cm/s) and ends (4.95 cm/s). This allows obtaining a fluid flow along the ureter due to the movement of the bolus that correspond with previous works results [10], [7].

3.3 INNER VOLUME

Figure 4 shows the inner volume of the inlet of the ureter. The lag in the start of the movement is due to the application of a time-dependent step in the volumetric force. After this moment, the movement begins and the total volume starts to increase rapidly. From 0.6 seconds, the increase of the volume starts to decelerate. However, additional longer simulations are needed to analyze properly the inner volume, because of this current short simulation (1.5 s) cannot assure stability and constant displacement of the urine flow (peristalsis bolus).

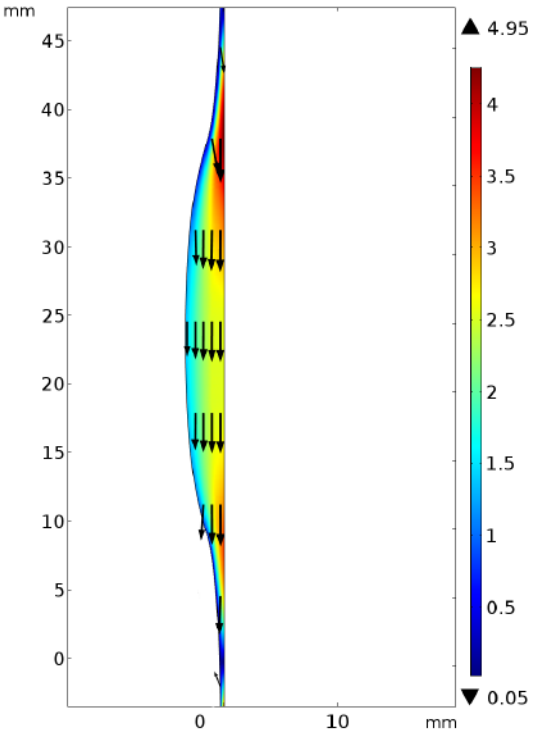

Figure 3: Velocity profile (cm/s) at 1.5 s simulation time.

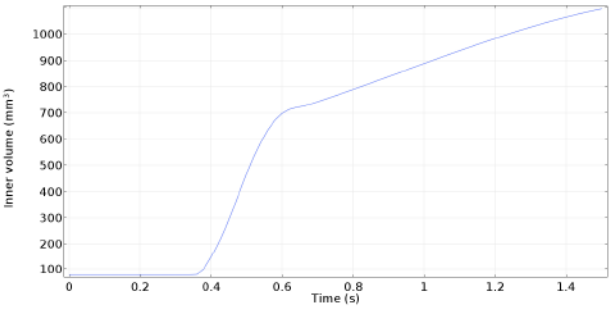

Figure 4: Inner volume (mm^3) in the inlet of the simulated section of the ureter.

3.4 PRESSURE

Figure 5 shows the pressure distribution along the ureter with the maximum and minimum pressures. This pressure is relative to atmospheric pressure as it can be deduced from the negative values. The expansion of the ureteral wall provokes a pressure variation. This variation is big enough, compared to atmospheric pressure, to provoke a minimum vacuum (-10 Pa) that fill the ureteral bolus with urine. Maximum and minimum pressure values are located in the proximal and distal part of the bolus, respectively. Maximum pressure value (13.44 Pa over atmospheric pressure) is place where the bolus ends, maximum contraction zone. On the other side, minimum pressure value (24.44 Pa under atmospheric pressure) is located where the ureteral wall begins to expand forming

the bolus.

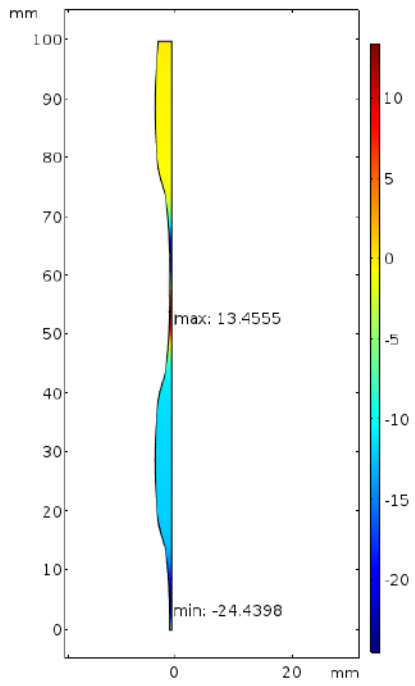

Figure 5: Pressure profile (Pa) at 1.5 *s* simulation time.

4 CONCLUSIONS

In this work a simulation of the peristaltic movement of the ureter was performed. The bolus was constructed from a closed ureter by the application of an expansive force obtaining a urinary bolus. The developed force model can generate a peristaltic movement more similar to the physiological one than previous in the literature. We have checked that peristaltic movement can generate a flow that does not depend on the pressure differences that exist along the ureter. Also, the velocity values obtained are within the physiological ranges obtained in previous works. However, there have been simulated only 1.5 *s* of peristalsis movement with a 0.3 *s* delay. So, our simulation time is not long enough to check how a bolus affects the next one, and how the flow can change.

Hence future simulations with finer mesh could facilitate a better resolution of the model. Also, redefined the force model with in vivo bolus geometries can generate a more precise peristaltic displacement. Finally, the addition of the stent model to the proximal zone of our model is necessary to evaluate the benefits of this new ureteral stent design.

Acknowledgement

This work was supported by the Ministry of Economy and Competitiveness (Carlos III Institute of Health PI16/01707)

References

[1] F. Osman *et al.*, "A novel videomicroscopic technique for studying rat ureteral peristalsis in vivo," *World Journal of Urology*, vol. 27, no. 2, pp. 265–270, 2009.

[2] F. C. Yin and Y. C. Fung, "Mechanical properties of isolated mammalian ureteral segments," *American Journal of Physiology – Legacy Content*, vol. 221, no. 5, pp. 1484–1493, 1971.

[3] D. P. Sokolis, "Multiaxial mechanical behaviour of the passive ureteral wall: experimental study and mathematical characterisation," *Computer Methods in Biomechanics and Biomedical Engineering*, vol. 15, no. 11, pp. 1145–1156, 2012.

[4] L. J. Cummings *et al.*, "The effect of ureteric stents on urine flow: Reflux," *Journal of Mathematical Biology*, vol. 49, no. 1, pp. 56–82, 2004.

[5] J. H. Siggers *et al.*, "Flow dynamics in a stented ureter," *Math Med Biol*, vol. 26, no. 1, pp. 1–24, 2009.

[6] J. C. Gómez-Blanco *et al.*, "Fluid Structural Analysis of Urine Flow in a Stented Ureter," *Computational and Mathematical Methods in Medicine*, vol. 2016, p. 7, 2016.

[7] B. Vahidi and N. Fatouraee, "A biomechanical simulation of ureteral flow during peristalsis using intraluminal morphometric data," *Journal of Theoretical Biology*, vol. 298, pp. 42–50, 2012.

[8] J. Jiménez-Lozano, M. Sen, and E. Corona, "Analysis of peristaltic two-phase flow with application to ureteral biomechanics," *Acta Mechanica*, vol. 219, no. 1, pp. 91–109, 2011.

[9] K. Yazdanpanh-Ardakani and H. Niroomand-Oscuii, "New approach in modeling peristaltic transport of non-Newtonian fluid," *Journal of Mechanics in Medicine and Biology*, vol. 13, no. 04, p. 1350052, 2013.

[10] B. Vahidi *et al.*, "A mathematical simulation of the ureter: effects of the model parameters on ureteral pressure/flow relations," *J Biomech Eng*, vol. 133, no. 3, p. 31004, 2011.

[11] T. A. Tasnub, G. Prashanta, and C. A. J., "A fluid-structure interaction (FSI)-based

numerical investigation of peristalsis in an obstructed human ureter," *International Journal for Numerical Methods in Biomedical Engineering*, vol. 0, no. 0, p. e3104, 2018.

[12] J. Mortensen *et al.*, "Renal Pelvis Pressure Flow Relationship in Pigs After Transsections of the Ureter," *Scandinavian Journal of Urology and Nephrology*, vol. 18, no. 4, pp. 329–333, 1984.

[13] COMSOL Multiphysics, "Theory for the Fluid-Structure Interaction Multiphysics Interface - Structural Mechanics Module," *Manual*, p. 454, 2008.

[14] A. Rassoli *et al.*, "Biaxial mechanical properties of human ureter under tension," *Urol J*, vol. 11, no. 3, pp. 1678–1686, 2014.